Layered double hydroxides as alternative catalysts for furan-based polyesters synthesis

Daniela Ramírez Espinosa[a], Laura Martí Montaner[a*], Alicia Monleón-Ventura[b*]

[a] *Instituto Tecnológico del Plástico (AIMPLAS), C/ Gustave Eiffel 4, 46980 Paterna, Valencia (Spain).*

[b] *Departament de Química Orgànica, Facultat de Química, Universitat de València*, Dr. Moliner 50, 46100 Burjassot, Valencia (Spain).

Abstract

The development of alternative systems for the synthesis of furan-based polyesters is essential for enabling sustainable and biobased polymer production. In this work, layered double hydroxides (LDHs) containing alternative divalent (Zn^{2+}, Sn^{2+}), trivalent (Sb^{3+}) and tetravalent (Ti^{4+}) metals to the traditional Mg^{2+} and Al^{3+} were synthesized and employed as catalysts for the production of poly(ethylene furanoate) (PEF) through a two-stage melt polymerization process. The X-ray diffraction data of the LDHs indicate the correct formation of crystalline structure. The catalytic performance of the LDHs was evaluated and compared to that of conventional metal catalysts. Zn/Sn/Al- and Mg/Al/Ti-based LDHs were efficient catalysts in the polymerization reaction. Interestingly, commercially available Mg/Al-based hydrotalcite afforded PEF with the highest molecular weight. Thermal properties of PEF were determined by thermogravimetric analysis and differential scanning calorimetry. All the synthesised polyesters are amorphous, exhibiting high Tg (83-87 ºC). The scalability and versatility of LDH-based catalysts were demonstrated by producing furan-based polyesters at different scales and with varying diol chain lengths from 4 to 6 carbons. The formation of poly(butylene furanoate) (PBF), poly(pentylene furanoate) (PPeB), and poly(hexylene furanoate) (PHF) was confirmed by IR and ^{1}H NMR. These results underscore the potential of LDHs as sustainable catalysts for advancing greener polymerization technologies.

Keywords: Layered double hydroxides (LDHs), hydrotalcite, poly(ethylene furanoate) (PEF), poly(ethylene terephthalate) (PET) alternative, polyester, catalysis, biobased furanoate polymer.

1. Introduction

Environmental challenges associated with the over-exploitation of fossil-based raw materials have prompted an urgent need for the development of more sustainable alternatives. Biobased polymers derived from renewable resources have emerged as plausible candidates for substituting petroleum-derived plastics [1]. Amongst the possibilities, 2,5-furandicarboxylic acid (FDCA) or its dimethyl ester derivative (2,5-dimethylfuranoate ester, FDME) have gathered worldwide commercial interest as building-blocks. They have been used as monomers with ethylene glycol (EG) in the synthesis of poly(ethylene furanoate) (PEF). This polymer has emerged as the most credible bio-based alternative to traditional fossil-based polyester poly(ethylene terephthalate) (PET) which is based on terephthalic acid (TPA), currently obtained from crude oil [2].

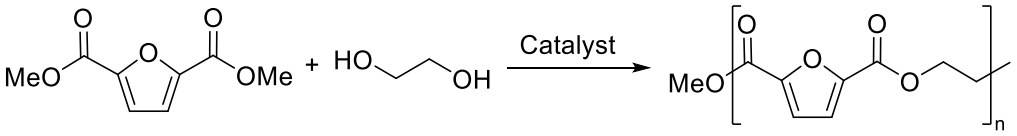

Scheme 1. Synthesis of poly(ethylene furanoate) (PEF) by polymerization of 2,5-dimethylfuranoate ester (FDME) and ethylene glycol.

PEF has shown improved performance properties compared to its terephthalic acid counterpart. In particular, it features very low CO_2 permeability, which has positioned this polymer as a perfect bio-based candidate for the packaging sector [3, 4, 5]. PEF also shows better O_2 barrier properties and higher tensile modulus. Additionally, the synthesis of PEF requires lower temperatures (up to 240 ºC) than the synthesis of PET (up to 250-280 ºC). In general, lower non-renewable energy use is required for its production [6, 7].

PEF's synthesis has been traditionally reported in the presence of catalysts such as antimuonium oxide, titanium alkoxides, or tin oxides following a two-stage melt polymerization approach which includes an initial (trans)esterification step and a second polycondensation reaction [8, 9]. These homogeneous catalysts are the subject of increasingly stringent regulations concerning their use in commercial products due to their potential toxicity [10].

In an effort to develop eco-friendly methodologies, ionic liquids have been explored as catalysts for the preparation of PEF. In 2019, Qu and coworkers utilized a Brønsted acidic ionic liquid for the efficient synthesis of PEF with high viscosity, but high decolouration of the polymer was found [11]. Recently, Guo's group successfully studied the catalytic performance of acidic-metal-based functional ionic liquids in the direct esterification of FDCA and EG [12]. Additionally, the catalyst-free synthesis of PEF has been recently reported in the presence of a 3.5 mol% diguaiacyl oxalate (DGO) chain extender, achieving the biobased polymer in Mn values as high as 51000 g/mol [13]. Other alternative protocols have been reported for the synthesis of PEF, such as the ring-opening polymerization using FDCA cyclic oligomers [14]. This process delivered bottle-grade PEF (Mn>30000 g/mol) within less than 30 min and could be positioned as an excellent competitive route for this biobased polymer. The short reaction times inhibit the by-product formation and the polymer discoloration. However, the reaction times for the preparation of the oligomers are similar to those required for the melt-stage polycondensation (from 7 to 10 h). Additionally, latter studies by Hoppe and coworkers revealed that cyclic oligomers can be potential migrants to food in contact with this material, thus, deeper studies to ensure the viability of this process are necessary [15].

The optimal procedure for the synthesis of PEF has not yet been described and, therefore, the search for alternative systems for the production of PEF is still imperative. In this context, layered double hydroxides (LDHs) have garnered attention as promising catalysts for the synthesis of polyesters [16]. LDHs present sheet structures with formula $M^{2+}_{1-x}\,M^{3+}_{x}\,(OH)_2](A^{n-})_{x/n} \cdot yH_2O$, where M^{2+} and M^{3+} are divalent and trivalent cations (M^{2+}= Mg, Zn, Ti, Fe, Ni, Co...; M^{3+}= Al, Ga, Fe…; A^{n-}= nitrates, carbonates, chlorides), where the tunability of the cations and anions makes these species perfect candidates for multiple applications. In particular, polyester synthesis, which comprises two processes (transesterification and polycondensation) requires the utilization of versatile catalysts capable of fostering both steps. In this sense, LDHs could be suitable catalysts for this purpose.

As heterogeneous catalysts, one of their advantages is their recoverability and recyclability. However, this is not always possible in polymer preparation. Therefore, the utilization of LDH and its incorporation in the final material should not affect its properties and performance. Kêdzierski and colleagues have investigated the application of LDHs as catalysts and nanofillers in the polytransesterification of dimethyl terephthalate with alkylene glycols [17]. The study concluded that zinc-aluminum hydrotalcite intercalated with anionic form of aminolauric acid [HT(ZnAl)ALA] can efficiently catalyse the transesterification process, increasing the rate of the reaction or lowering its temperature when compared to the reaction with conventional organotin catalyst and leading to a transparent polyester resin.

Amongst others, LDHs have attracted wide attention due to characteristics such as their tunability, environmental compatibility, as well as their unique structural properties, including high surface area, basicity, and thermal stability, making them a compelling alternative to conventional metal-based catalysts. In addition, they stand out for their easy synthesis, low cost, and long-time durability. These properties are ideal for polymer industry applications, especially taking into consideration that some typical metals in LDHs are not strictly limited by food contact regulation. LDHs allow the possibility of combining different metals in one single catalytic system, which can be convenient in polymerization processes comprising two types of reactions, such as transesterification and polycondensation. In addition, there is an imperative need to find a catalytic system that overcomes one of the main drawbacks in the synthesis of furan-based polyesters such as the high discoloration. Therefore, to expand the repertoire of suitable and greener catalysts for biobased furan-based derived catalysts and to open up for new possibilities in the synthesis of bioesters and biobased copolymers, this work has investigated for the first time the applicability of LDH as catalysts in the synthesis of poly(ethylene furanoate) (PEF) and other furan-based polyesters whose properties have been studied and compared.

2. Experimental

2.1. Materials

Ethylene glycol ≥99.7% (VWR), 2,5-furandicarboxylic acid dimethyl ester 98% (FDME) (Biosynth), 1,4-butanediol 99% (Sigma Aldrich), 1,5-pentanediol ≥97% (Sigma Aldrich), 1,6-hexanediol for synthesis (Sigma Aldrich) were used for polyesters synthesis.
Hydrotalcite MgO/Al_2O_3 ratio = 4-5 (Sigma Aldrich), Hydrotalcite $[Al_2Mg_6(OH)_{16}]CO_3 \cdot 4.45H_2O$ (Kisuma), $Al(NO_3)_3 \cdot 9H_2O$) ≥95% (Merck), $Zn(NO_3)_2 \cdot 6H_2O$ ≥98% (Sigma Aldrich), $SbCl_3$ ≥99.0% (Sigma Aldrich), Na_2CO_3 ≥99.5% (Sigma Aldrich), NaOH ≥98.0% (Scharlab), $Mg(NO_3)_2 \cdot 6H_2O$ ≥99.0% (Sigma Aldrich), $SnCl_2 \cdot 2H_2O$ 98% (Sigma Aldrich), $TiCl_4$ 99,9% (Sigma Aldrich), $ZnCl_2$ 97% (Sigma Aldrich) were used for catalyst production.

2.2. Catalysts preparation

Different hydrotalcite based on zinc [18], magnesium [19, 20], tin [21], antimuonium [22], aluminium [21] and titanium were prepared by precipitation of soluble salts of di and trivalent cations by alkaline solutions at variable pH or by coprecipitation at constant pH [23, 24]. The molar ratios used were the following: LDH01 (Zn/Sb/Al=1.51:1.5:1) [22], LDH02 (Zn/Al/Sb=3:0.8:0.2) [22], LDH03 (Zn/Sn/Al=1.51:1.5:1) [26], LDH04 (Zn/Sn/Al=4.66:0.60:0.71) [23], LDH05 (Zn/Al/Ti=7.69:1:0.85) [25], LDH06 (Mg/Sn/Al=2.99:0.1:0.91) [26], LDH07 (Mg/Sn/Al=3:0.3:0.7) [266], LDH08

(Mg/Al/Ti=2.67:0.98:0.34) [30], LDH09 (Mg/Al/Ti=2.89:0.57:0.55) [30], LDH10 (Mg/Al/Ti=2.99:0.91:0.1) [30], LDH11 (Zn/Ti=3.88:0.45) [27], LDH12 (Zn/Ti=3.84:0.39) [27], LDH13 (Zn/Mg/Al=1.50:1.50:1) [28], LDH14 (Zn/Mg/Al=4.35:4.35:1) [28], LDH15 (Zn/Al=7.68:1) [29], LDH16 (Zn/Al=16.23:1) [29] and LDH17 (Mg/Al=2.96:1.05) [30].

To this end, two aqueous solutions, a solution of the metal nitrates or metal chloride and a mixed solution of NaOH and Na_2CO_3 precipitant, were added dropwise to 100 mL of deionized water under vigorous stirring. The mixed solution was conducted at a pH range of 9.0–10.0 (pH was adjusted to 10 in all cases except for Zn/Al/Ti-based LDH, where the pH was adjusted to 9, as previously reported [25]). The product was then transferred into the Teflon-coated stainless-steel autoclave for hydrothermal treatment at a range of 40-120 °C for 10 h-24 h under autogenous water vapour pressure. After the hydrothermal treatment, the precipitate was filtered and washed with deionized water. The filter cakes were dried overnight at 60 °C.

2.3. Catalyst characterization

Powder X-ray diffraction (XRD) patterns were recorded on a Bruker model D8 ADVANCE A25 ray diffractometer with CuKα radiation in the range of $5°<2\theta<80°$.

Scanning electron microscopy (SEM) of the LDHs was performed with a PHENOM WORLD PRO X equipment (see Supporting Information for further details).

The basic strength of LDHs was determined qualitatively by identifying colour change of Hammett indicators including [31]: methyl red ($H_- = 5.3$), bromothymol blue ($H_- = 7.3$), phenolphthalein ($H_- = 9.5$), and 2,4-dinitroaniline O ($H_- = 15.0$). These indicators were added to the dry MeOH to prepare a 1.0×10^{-5} M solution. LDHs (0.050 g) were then added to 1 mL of the solution. The solutions were then stirred for 2 h to reach equilibrium. The strength of the base sites was qualitatively analysed by observing the colour of the solution.

2.4. Polymer synthesis

The furan-based polyesters were prepared by the two-stage melt polycondensation method (transesterification and polycondensation). For the polymer synthesis at a 5-gram scale, a glass reactor was charged with FDME (27.15 mmol), the diol (2.2 equivalents), and the catalyst (0.04% w/w FDME for conventional metal catalysts and 1% for LDH). The air of the system was evacuated, and it was filled with N_2. The reaction mixture was heated to 180 ± 5 °C and this temperature was kept for 2 h. After this time, the first step (transesterification) was considered complete since MeOH was not being formed. MeOH was removed from the reaction mixture by distillation and collected in a graduated cylinder. Then, the reaction temperature was raised to 230 °C gradually while the pressure is reduced gradually to 3-5 mbar (over 15 min) for the second polycondensation step to remove the excess diol and traces of remaining MeOH. The reaction is maintained at 230 ± 5 °C and low pressure for 5 h.

To check and ensure the temperature of the crude reaction mixture, a thermocouple data logger was used. When the polycondensation reaction was completed, the furan-based polyesters were removed from the glass reactor and milled for characterization.

The 30-gram scale reaction was performed in a 250-mL 3-neck glass reactor coupled with rotatory stirring by means of an overhead Hei-Torque laboratory stirrer adapted to a stainless steel or PTFE half-moon impeller.

2.5. Polymer characterization

Differential Scanning Calorimetry (DSC) was performed on a Differential Scanning Calorimeter 214 POLYMA calibrated with high purity standards and following the standard UNE-EN ISO 11357-1 and UNE-EN ISO 11357-3. Samples of 1-2 ±0.1 mg were sealed in aluminum pans under nitrogen with a heating rate of 10°C/min in the temperature range of -50°C–200°C.

The molecular weight distribution of the samples was analyzed by Gel Permeation Chromatography (GPC) on a Waters 2525 equipment connected to a PDA Waters detector model 2998 at 210 nm wavelength analysis. The samples were prepared by the dilution of 10 mg of the polymer into 5 mL of 1,1,1,3,3,3-hexafluoro-2-propanol (HFIP) 0.05 M of sodium trifluoroacetate (NaTFA) was injected and chromatographed with a flow of 1 mL/min. Phenogel 5 U lineal column (7.8 mm ID and 300 mm length) at 25 ºC was used. Molar mass average and distributions were calculated against polymethylmethacrylate (PMMA) standards in a third-order calibration line. The chromatogram shows the number average molecular weight (Mn), the weight average molecular weight (Mw) and the polydispersity index (PDI).

Thermogravimetric analysis (TGA) measurements were made using a TA Instruments TGA Q5000. A 10–20 mg sample was spread out on a platinum pan. Degradation process has been performed in the temperature range from 25 to 900 ºC, nitrogen atmosphere with gas flow rate of 40 mL/min, and heating rate of 20 ºC/min.

NMR spectra were run at 300 MHz in a Bruker AvanceIII 300 spectrometer for ^{1}H NMR using residual non-deuterated solvent (trifluoroacetic acid, CF_3COOD – TFA-d) as internal standard (δ 11.5 ppm). Chemical shifts (δ) are given in part per million (ppm). ^{1}H-NMR spectra were recorded at room temperature.

Infrared spectroscopy (FTIR) was done according to internal procedure QE-15 in a Fourier Transformed Infrared Spectrophotometer NICOLET 6700 using the method Reflection in Smart Orbit with diamond glass. 10 scans were applied with a 4 cm^{-1} resolution and a scanning range of 4000-400 cm^{-1}. The sample was prepared by grinding to a powder.

3. Results and Discussion

3.1. Layered double hydroxides X-ray powder diffraction

A collection of 17 layered double hydroxides was prepared for the polymerization study. LDHs were based on common cations Mg^{2+}, Al^{3+} and Zn^{2+} and the anions, usually CO_3^{2-} or water. The incorporation of other cations such as Sb^{3+}, Sn^{2+} and Ti^{4+} was based on previously known metals capable of catalysing the transesterification and polycondensation reactions in polyester synthesis [6, 9].

The XRD patterns of LDH with different metal combination are shown in Fig. 1a.

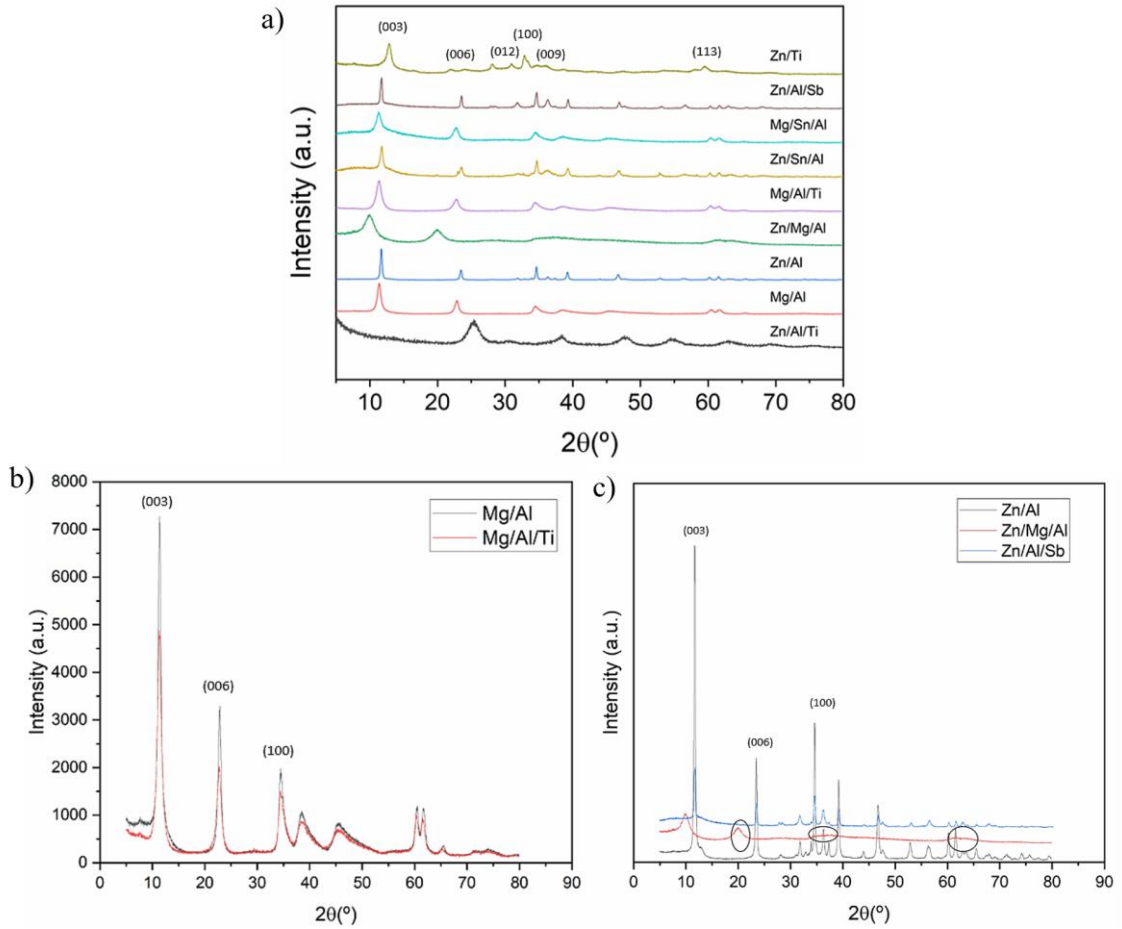

Fig. 1. XRD patterns of a) synthesised hydrotalcites; b) hydrotalcite Mg/Al and Mg/Al/Ti; c) comparative of hydrotalcites Zn/Al, Zn/Al/Mg and Zn/Al/Sb.

Fig. 1a illustrates the powder XRD pattern for Zn/Ti LDH. A strong reflection (003) was observed for the sample. XRD pattern also show the reflections of (006), (009), (100), (012) and (113) which can be indexed to typical LDH materials [32].

The XRD pattern of Zn/Al/Ti LDH (Fig. 1a) shows high crystallinity, which could be related to a low titanium content in the sample, thus avoiding a large distortion in the layers, associated to the increase of the positive charges of the layers leading to interlayer repulsion.

Concerning the Mg/Al and Mg/Al/Ti hydrotalcites, it can be observed that a crystalline structure characteristic of this type of material is obtained.[30] However, the crystallinity decreases when Ti^{+4} is incorporated in the synthesis, i.e. for the Mg/Al hydrotalcite the peak (003) presents an intensity of 7000 a.u. and the peak (100) an intensity of 2000 a.u. while the hydrotalcite Mg/Al/Ti presents an intensity of 2000 a.u. for peak (003) and 1500 a.u. for peak (100). u. and the peak (100) has an intensity of 2000 a.u. while the Mg/Al/Ti hydrotalcite has an intensity of 2000 a.u. for the peak (003) and an intensity of 1500 a.u. for the peak (100). (Fig. 1b).

The XRD patterns for both the Mg/Al and the Mg/Sn/Al solid (Fig. 1a) are typical of layered clay minerals. The XRD patterns of the hydrotalcites Zn/Al, Zn/Al/Sb and Zn/Mg/Al can be seen in Fig. 1a, where it is demonstrated that these catalysts show the characteristic diffraction peaks corresponding to the (003), (006), (012) and (100) crystalline planes [18, 21, 22].

The presence of sharp, narrow and symmetric diffraction peaks in the Zn/Sn/Al XRD pattern indicates a well-crystallized sample with a low and stable baseline. And the high peak around 11.6° (Fig. 1a) support that the LDH Zn/Sn/Al has a hexagonal crystal structure, typical for these materials as reported in the literature [244].

As can be seen from the Fig. 1c, the two samples with similar XRD diffraction patterns manifest that the introduction of antimony does not alter the basic structure of LDH. While the incorporation of magnesium into the Zn/Al hydrotalcite did affect the crystalline phase of the material, by changing the crystallisation of the Zn/Mg/Al forming the distinctive periclase-crystal structure of magnesium oxide, with the characteristic planes (circled in Fig. 1c).

To obtain qualitative information about the strength of the basic sites of selected LDHs, four Hammett indicators were employed: methyl red (H_ = 5.3), bromothymol blue (H_ = 7.3), phenolphthalein (H_ = 9.5), and 2,4-dinitroaniline O (H_ = 15.0). LDHs containing different cations were chosen (see Table 2 and Figure S 9). The base strengths were determined from the colour changes in the indicators. A high H_ value of the indicator indicates high base strength. When utilising methyl red all LDHs shows solutions showed yellow (red below 4.4, orange between 4.4 and 6.2 and yellow above 6.2), indicating base properties with an H_ of 6.2 or higher. When employing bromothymol blue with an H_ of 7.3, the LDHs showed different blue intensities; however, all of them had base properties (H_ > 7.3). When using phenolphthalein indicator with an H_ of 9.5, different colours were observed. Colourless indicates acid properties, whereas pink indicates base properties., LDH02, LDH11 and LDH18 were colourless. LDH04 and LDH15 showed a light pink colour. LDH10 and LDH06 showed a more intense pink colour. Based on these observations, LDH02, LDH11 and LDH18 have H_ values between 7.3 and 9.5, the H_ values of LDH04 and LDH15 were around 9.5, which is the H_ of phenolphthalein. Finally, all LDHs showed a yellow colour with 2,4-dinitroaniline, indicating acid properties. Therefore, LDH10 and LDH06 have H_ values between 9.5 and 15.

3.2. LDH-catalysed furan-based polyester synthesis

PEF was synthesized following a two-step polycondensation procedure where the viability of different layered double hydroxides as catalysts was evaluated. The utilization of FDCA as the monomer presents several drawbacks [33]. It discolours over time due to its instability, it has a high melting point (> 300 ºC), which makes the polymerization process harsh, and it is poorly soluble in organic solvents. Therefore, we found it convenient to develop this work with its dimethyl ester (FDME) following a transesterification and polycondensation approach.

Some reaction parameters were established according to the requirements of the process and previous reports in literature [34, 35]. The transesterification reaction must be carried out under the boiling point of EG and at a temperature where both FDME and EG are in liquid phase forming a homogeneous solution. In this step, the temperature must also allow the evaporation of the MeOH formed in the condensation reaction between the FDME and the EG. With these considerations in hand, the transesterification was performed with 5 g of FDME at 180 ºC for 2 h under N_2 atmosphere. In the polycondensation reaction, on one hand, excess of EG must be removed from the reaction mixture and, on the other hand, PEF has to be above its melting temperature. However, reaching too high temperatures leads to the coloration of the final material. Taking this into account, this second step was carried out at 230 ºC under vacuum as indicated in Table 1.

An excess of EG is needed for the success of the polymerization [36]. Nevertheless, a large amount of unreacted EG could hinder the polycondensation step. A molar relationship of FDCE:EG of 1:2.2 equivalents was applied.

As a starting point and for comparison reasons, the reaction was initially performed in the presence of traditional metal-based catalysts for polyester synthesis: Sb_2O_3, Bu_2SnO, $Ti(OnBu)_4$ (Table 1, Entries 1 to 3). Number average molecular weight and weight-average molecular weight were obtained for the synthesized PEF. $Ti(OnBu)_4$ afforded PEF in highest Mn and Mw. However, the main drawback of this catalyst is its sensitivity to air and moisture and the discolouration that it produces in polyester (Fig. 3).

Once these results were obtained for latter comparison, our study began with the utilization of 1 mol% of zinc and aluminium-based layered double hydroxides having antimuonium-, tin- and titanium in their structures (LDH01 to 05) (Table 1, Entries 4-8). The catalytic amount of these heterogeneous LDH catalysts is 25 times higher than the catalytic load utilizing conventional metal catalysts. Zn/Sb/Al-LDH01 and Zn/Sb/Al-LDH02, with different metal ratio, led to PEF in low molecular weights (Mn and Mw). A similar result was achieved when Zn/Sn/Al-LDH03 was utilized. On the contrary, when the proportion of aluminium was increased (Zn/Sn/Al-LDH04), PEF was obtained in comparable results to those with conventional metal catalysts, although the polydispersity index was higher. Zn/Al/Ti-LDH05 catalysed the synthesis of PEF more efficiently than Sb-based LDH01 and LDH02; however, these results were far from the objective and did not reach the Mw obtained with LDH04. Next, a series of magnesium and aluminium-based LDHs containing tin or titanium were evaluated. Mg/Sn/Al-LDH06 and Mg/Sn/Al-LDH07 resulted in short polymer chains. Mg/Al/Ti-LDH08, Mg/Al/Ti-LDH09 and Mg/Al/Ti-LDH10, having a similar composition, led to good results; however, Mg/Al/Ti-LDH10, having a lower content of titanium catalysed the polymerization of FDME and EG significantly better. Then, Zn/Ti-LDH11 was examined. It led to good molecular weights, although lower than LDH10. With Zn/Mg/Al-LDH13 a low degree of polymerization was achieved. However, LDH14, where the proportion of aluminium was decreased, longer PEF chains were obtained. Zn/Al-based LDHs, LDH15 and LDH16, also performed satisfactorily in the polymerization reaction. Finally, Mg/Al-based LDHs were evaluated. Satisfyingly, commercially available hydrotalcites HT-comm Aldrich ($Mg_6Al_2(CO_3)(OH)_{16} \cdot 4H_2O$) and HT Kitsuma led to PEF in high Mn and Mw, comparable to those obtained with conventional metal catalysts.

Table 1. Synthesis of PEF by a two-stage melt polymerization from 5 g of FDME and EG with different catalysts.

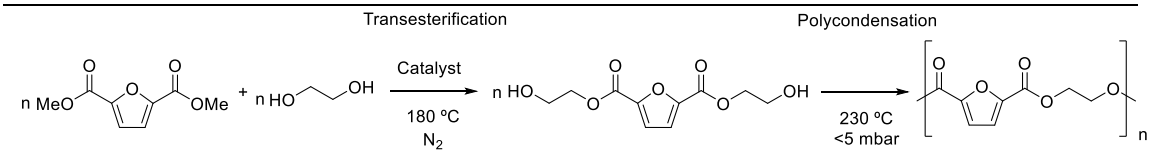

Entry	Catalyst	Metal molar ratio in LDH	Mn (g·mol^{-1})[a]	Mw (g·mol^{-1})[b]	PDI (Mw/Mn)[c]
1	Sb_2O_3	Not applicable	23633	47136	1,99
2	Bu_2SnO	Not applicable	23530	40601	1,72
3	$Ti(OnBu)_4$	Not applicable	25350	61694	2,43
4	LDH01	Zn/Sb/Al=1.51:1.5:1	8214	13581	1.65
5	LDH02	Zn/Al/Sb=3:0.8:0.2	4580	16330	3,57
6	LDH03	Zn/Sn/Al=1.51:1.5:1	3288	18420	5,60

7	LDH04	Zn/Sn/Al=4.66:0.6:0.71	17490	45705	2,61
8	LDH05	Zn/Al/Ti=7.69:1:0.85	10919	20218	1,85
9	LDH06	Mg/Sn/Al=2.99:0.1:0.91	2809	8812	3,14
10	LDH07	Mg/Sn/Al=3:0.3:0.7	4031	11668	2,89
11	LDH08	Mg/Al/Ti=2.67:0.98:0.34	12399	21338	1,72
12	LDH09	Mg/Al/Ti=2.89:0.57:0.55	12243	20323	1,66
13	LDH10	Mg/Al/Ti=2.99:0.91:0.1	19241	47581	2,47
14	LDH11	Zn/Ti=3.88:0.45	18012	36934	2,05
15	LDH12	Zn/Ti=3.84:0.39	17493	33361	1,91
16	LDH13	Zn/Mg/Al=1,50:1,50:1	5272	7841	1,49
17	LDH14	Zn/Mg/Al=4.35:4.35:1	12597	24967	1,98
18	LDH15	Zn/Al=7.68:1	19002	35384	1,86
19	LDH16	Zn/Al=16.23:1	17762	32408	1,82
20	LDH17	Mg/Al=2.96:1.05	17785	38332	2,16
21	LDH18	Mg/Al – Aldrich Commercial	21808	55177	2,53
22	LDH19	Mg/Al - Kisuma	19097	44759	2,34
23[d]	LDH18	Mg/Al – Aldrich Commercial	26292	52259	1,99

[a] Number average molecular weight (Mn). [b] Weight average molecular weight (Mw). [c] Polydispersity index (PDI) of PEF. d High-scale synthesis of PEF utilizing 30 g of FDME.

A graphical analysis of the results in comparison with the Mn (Fig. 2a) and Mw (Fig. 2b) obtained with Sb_2O_3, Bu_2SnO and $Ti(OnBu)_4$ indicates that commercial LDH18 gives PEF in good Mn above 20000 g/mol, similar to the Mn achieved with conventional catalysts. In addition, LDH18 leads to higher Mw (>55000 g/mol) than Sb_2O_3 and Bu_2SnO (<50000 g/mol). LDH04, LDH10 and LDH19 also stand out amongst other LDH and provide PEF in high Mw (>40000 g/mol). With these results in hand, we considered a deeper characterization of the PEF synthesised with LDH04, LDH10 and LDH18, which present different metal composition and demonstrate to be suitable catalysts for polyester polymerization.

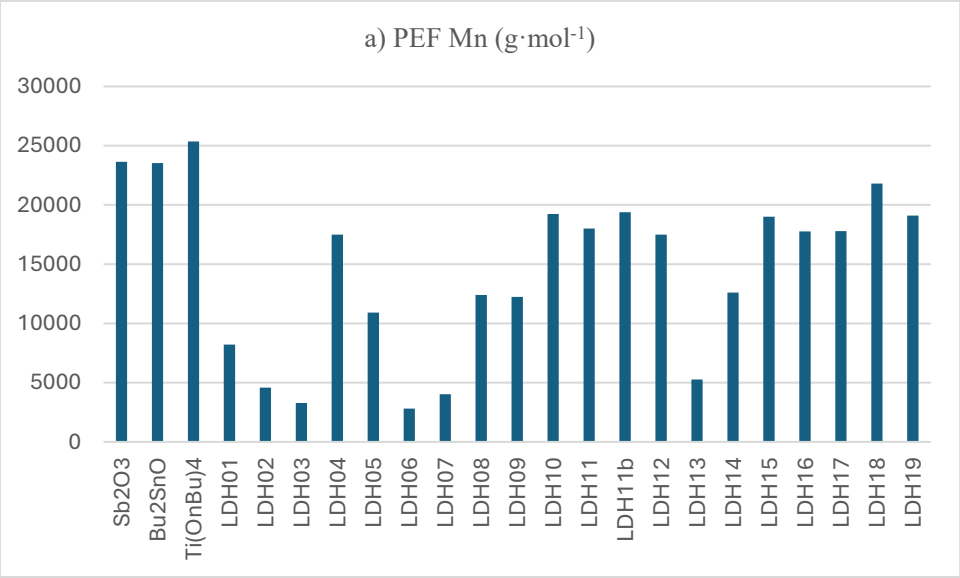

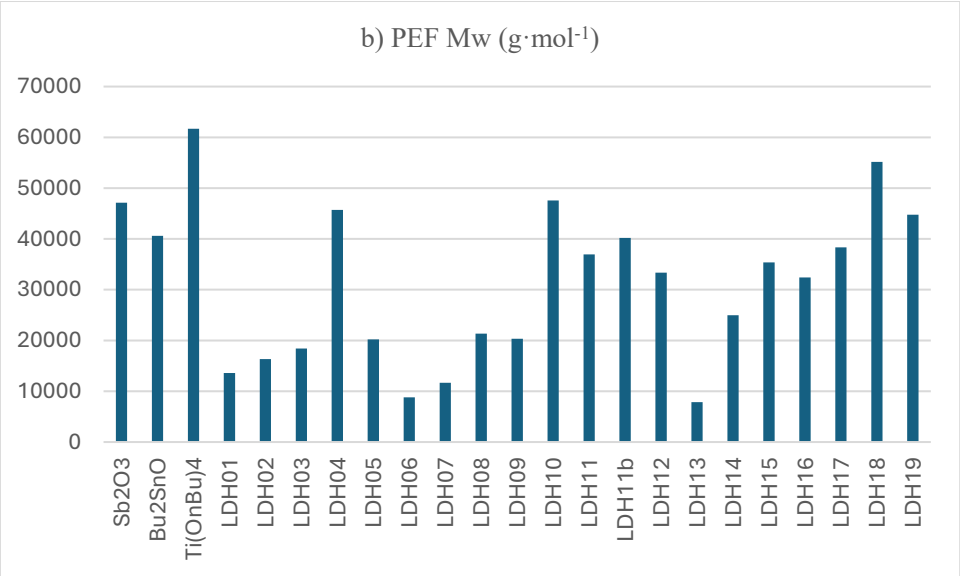

Fig. 2. a) Number average molecular weight (Mn) comparison, and b) weight average molecular weight (Mw) comparison of PEFs obtained through different catalysts.

When comparing the basic strength of the surface of selected LDHs with the molecular weights achieved with each of them, there is not a clear correlation between the estimated strength of the basic sites and the catalyst activity (Table 2). As an example, Mg/Sn/Al-based LDH06 which showed a H_ value between 9.5 and 15 led to very low molecular weight, whereas Mg/Al/Ti-based LDH10 showing similar basic strength provided PEF in high Mn and Mw. The presence of CO_3^{2-} anions within the LDH interlayers could be interfering with the material's basicity. It is also worth noting that the presence of metals that can act as Lewis acids in the structure of the LDHs could be providing additional catalytic activity to these materials, since the coordination of these metals to the oxygen of the carbonyl groups in the FDME can enhance the electrophility of the carbonyl group and favour the reaction with ethylene glycol. Therefore, the activity of the LDHs may be affected by the Lewis acidity of the metals as well.

Table 2. Base strength of selected LDHs.

LDH	Metals	Base strength	PEF Mn (g·mol^{-1})	PEF Mw (g·mol^{-1})
LDH02	Zn/Al/Sb	7.3-9.5	4580	16330
LDH04	Zn/Sn/Al	9.5	17490	45705
LDH06	Mg/Sn/Al	9.5-15	2809	8812
LDH10	Mg/Al/Ti	9.5-15	19241	47581
LDH11	Zn/Ti	7.3-9.5	18012	36934
LDH15	Zn/Al	9.5	19002	35384
LDH18	Mg/Al	7.3-9.5	21808	55177

The PEF samples synthesized through conventional catalysis exhibited discoloration, particularly those produced using Sb and Ti catalysts (Fig. 3). The polymer obtained with Sn demonstrated minimal discoloration. Similar results were reported by Terzopoulou et al. [37], where the utilization of dibutyltin(IV) oxide, tin(II) 2-ethylhexanoate, titanium(IV) isopropoxide and tetrabutyl titanate led to brown to dark brown colorations. Notably, hydrotalcite catalysis herein studied yielded PEF with the least discoloration, achieving the most favourable colour among the samples. It is worth noting that, overcoming the drawback of high discoloration in the synthesis of PEF is an important advantage in the utilization of LDH catalysts.

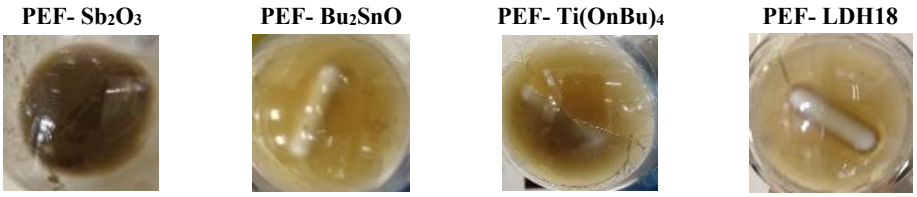

Fig. 3. PEF samples colour comparison.

FTIR spectrum of PEF sample obtained by LDH18 catalysis confirms that the polymerization was successful (**¡Error! No se encuentra el origen de la referencia.**). The weak bands near 3121-3154 cm^{-1} correspond to the out-of-plane and in-plane CH stretching of the furan ring. The strong absorption peak related to the C=O stretching appears at 1719-1730 cm^{-1}. The band at 1576 cm^{-1} is associated with the aromatic C-C bending vibrations. The characteristic C-O ester stretching vibration is at 1266 cm^{-1}. A furan ring breathing band is identified at 1133 cm^{-1} and 1017-1023 cm^{-1} and the peaks at 955-970 cm^{-1} and 836-856 cm^{-1} are related to furan ring bending.

The catalytic effect of commercial Double Layered Hydroxide, LDH18, in the polymerization of FDME and ethylene glycol was evaluated at a 30-gram scale (Table 1, Entry 23). The evolution of the transesterification step was controlled by the measurement of the MeOH formed. This first step required 3 h instead of 2 h to be completed. Then, the polycondensation step was allowed to occur for 7 h, when the maximum torque values were achieved. At 30 g, Mn increased to 26292 g/mol, while Mw decreased slightly to 52259 g/mol, with a lower PDI of 1.99. This indicates a more uniform molecular distribution in the larger scale synthesis, albeit with a slight reduction in Mw. This demonstrates the scalability of the process and the potential utilization of LDHs for industrial applications.

The thermal properties of the synthesized PEF samples were studied by DSC. Fig. 4a and 4b depicts the second and first heating, respectively, scans of amorphous PEF samples obtained by the polymerization catalysed with conventional catalysts (Sb_2O_3, Bu_2SnO, $Ti(OnBu)_4$) and selected LDHs (LDH04, LDH10 and LDH18). Fig. 4b indicate that the material is amorphous as it has a cold crystallization (exotherm) prior to fusion at first heating. The samples PEF-Sb_2O_3 and PEF-$Ti(OnBu)_4$ stand out for their high melting points (208.8 ºC and 210.3 ºC, respectively) during first heating and high enthalpies of fusion (52.4 J/g and 39.5 J/g), indicating good thermal stability. PEF-Bu_2SnO exhibits a low Tm (150.7 ºC), PEF-LDH04 presents a negative ΔHm, suggesting possible unusual crystallisation processes. Both PEF-LDH10 and LDH-18 show lower melting points during the first heating possibly associated with the presence of oligomers. Fig. 4a (second heating) confirmed the amorphous structure of all synthesized PEFs, with glass transitions (Tg) between 83.2 ºC and 86.8 ºC.

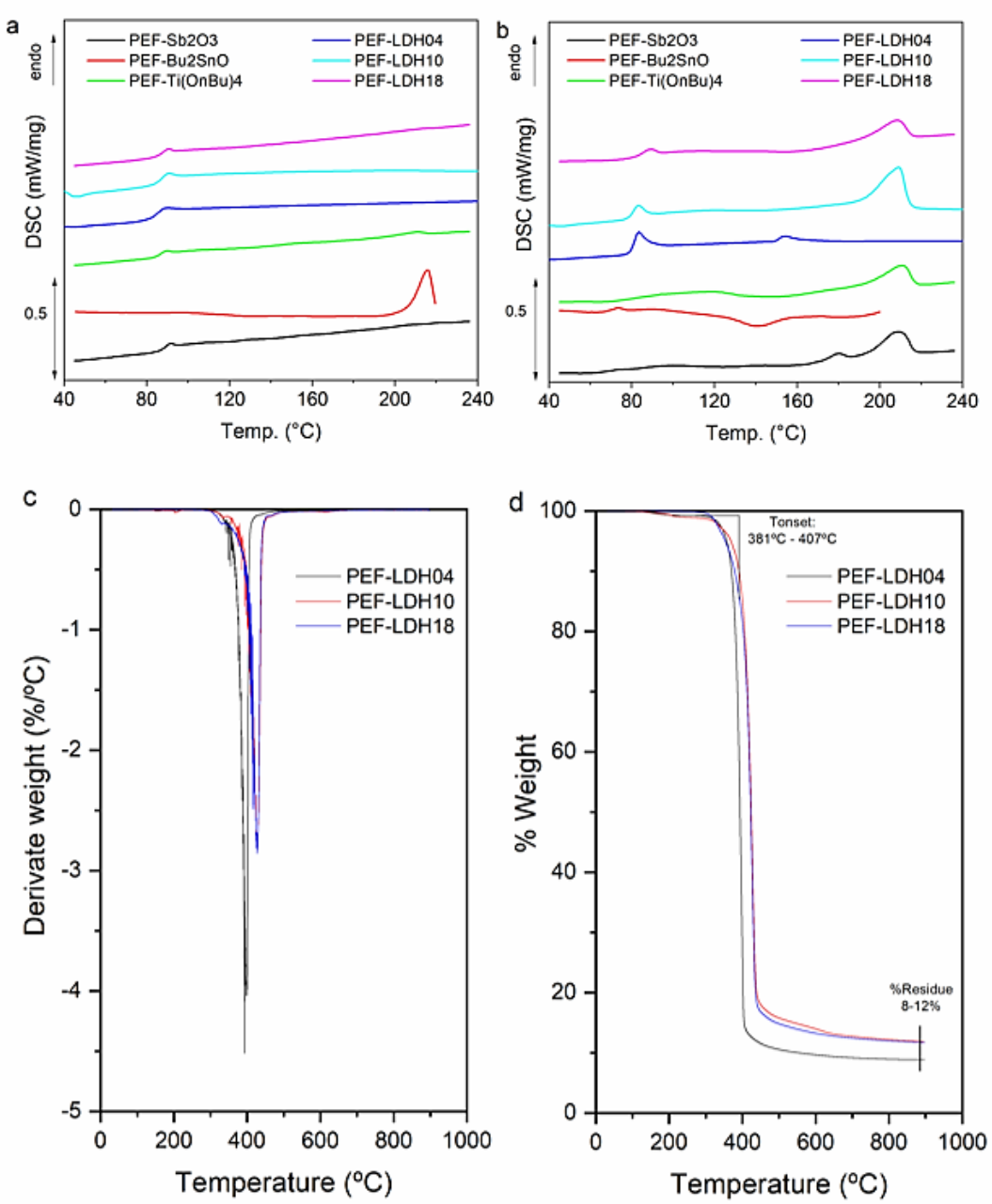

Fig. 4. Thermal properties of PEFs by a) 2nd heating DSC scan, b) first heating DSC scan, c) DTG curves, d) TGA curves obtained through different catalysts.

Fig. shows the derivation of mass in relation to time (first derivative of TGA) DTG (c) and TGA (d) curves of the PEFs obtained using different catalysts under nitrogen atmosphere. The degradation temperature for PEF-LDH04 starts at 381.8 ºC. But weight loss does not take place before 300 ºC, which indicates that polymer exhibits excellent thermal stability and the weight of residues at 900 ºC is around 8%. Similarly, the samples PEF-LDH10 (Tonset: 407.4 ºC, 12.5%) and PEF-LDH18 (Tonset: 405.1 ºC, % residue: 11.9%) do not show significant weight loss at low temperatures, i.e. they have a similar thermal stability to PEF-LDH04.

In all three materials, decomposition occurs in the range of 300-500 °C, possibly associated with the decomposition of the organic matrix. This indicates that the different catalysts used in the synthesis do not drastically affect the overall thermal stability of the PEF. Fig. (c) shows slight variations in the intensity and position of the weight loss peaks (derivative). These differences

could be due to residual effects of the catalysts influencing the degradation kinetics. Fig. 4 (d) reveal that the amount of residual material above 800 °C is low (less than 13%) and almost identical for two materials (PEF-LDH10 and PEF-LDH18). However, the sample PEF-LDH04 shows 8% of residual material, this difference between the samples could be due to variations in the composition of LDHs. It can be concluded that the small differences observed may reflect modifications in the polymer microstructure (such as branching or defects), induced by the catalysts.

To further demonstrate the applicability of LDHs in the synthesis of furan-based polyesters, the polymerization with FDME and other diols was performed. 1,4-butanediol, 1,5-pentanediol and 1,6-hexanediol were tested to afford poly(butylene furanoate) (PBF), poly(pentylene furanoate) (PPeB), and poly(hexylene furanoate) (PHF) [38]. Results are presented in Table 3. PBF and PHF were obtained in low to moderate Mn and Mw, respectively, whereas PPeF was synthesized in high Mn and Mw. This could be due to the odd-even change of the number of the methylene groups in the monomeric unit of diol, which is known as the odd-even effect [39].

Table 3. LDH18-catalysed synthesis of furan-based polyesters with different diols.

Entry	Diol	Mn ($g \cdot mol^{-1}$)	Mw ($g \cdot mol^{-1}$)	PDI (Mn/Mw)
1	Ethylene glycol	21808	55177	2,53
2	1,4-butanediol	1829	7564	4,13
3	1,5-pentanediol	26211	61194	2,34
4	1,6-hexanediol	15508	32202	2,08

Furan-based polyesters (PEF, PBF, PPeF and PHF) were characterized by IR (Figure S 11) and ^{1}H NMR (Fig. 5). The peaks patterns of the IR spectra of PBF, PPeF and PHF are in accordance with the pattern of PEF (Figure S 10). They all show the characteristic signals of the CH stretching of the furan ring (3115-3115 cm^{-1}) and a band around 2700-2950 cm^{-1} related to the out-of-plane stretching of alkyl methylene groups, whose intensity grows as the number of methylene groups increases. All samples have the strong absorption peak associated with the C=O stretching vibration (around 1715 cm^{-1}), the C=C stretching vibration (around 1575 cm^{-1}) and the ester C-O stretching vibration (around 1265 cm^{-1}), thus corroborating the successful polymerization.

The ^{1}H NMR spectra shown in Fig. additionally confirm the structure of the polyesters. For PEF, the chemical shifts of CH (a) in the furan ring and CH_2 (b) from ethylene glycol appear at 7.40 ppm and 4.82 ppm, respectively. The tiny chemical shifts at 4.71 and 4.19 ppm can be attributed to CH_2 (b, c) in outer units of the polymer chain. For PBF, the CH signal of the furan ring appears at 7.68 ppm. The methylene groups (c) directly bonded to the O of the ester can be found at 4.87 ppm as a broad singlet, and the peak at 2.34 ppm corresponds to the CH_2 (d). In PPeF spectrum, the CH in the furan ring is at 7.66 ppm, the triplet at 4.81 showing a coupling constant of 6.58 Hz can be attributed to CH_2 (e). The peaks of methylene groups f and g appear as multiplets at 2.19-2.29 ppm and 1.91-2.00 ppm, respectively. Finally, for PHF, the chemical shift of the CH in the furan ring is at 7.45 ppm, the multiplet at 4-57-4.61ppm corresponds to methylene groups h. This multiplet can be formed as the overlap of two triplets attributed to methylene h in inner (*) and outer (.) chains of the polymer. Then, CH_2 (i) and CH_2 (j) signals appear at 1.98 and 1.67 ppm, respectively.

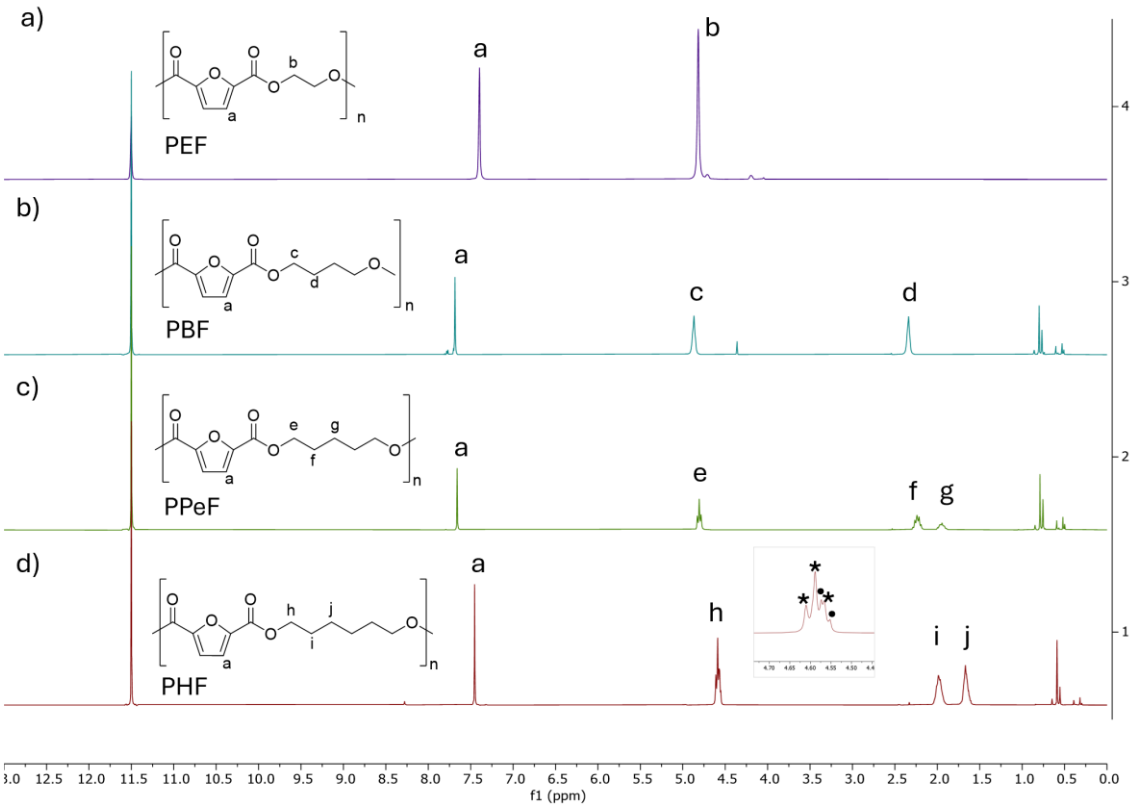

Fig. 5. [1]H NMR spectra of a) poly(ethylene furanoate) (PEF), b) poly(butylene furanoate) (PBF), c) poly(pentylene furanoate) (PPeB), and d) poly(hexylene furanoate) (PHF) in TFA-d (referred at 11.5 ppm).

Conclusions

The development of alternative systems for the synthesis of furan-based polyesters is necessary to achieve sustainable processes capable of affording biobased polymers in the appropriate characteristics. Herein, a collection of easily achieved and stable layered double hydroxides has been synthesised. The X-ray diffraction data of the LDHs indicate the correct formation of crystalline nanocomposite. These LDHs were utilized as catalysts for the synthesis of poly(ethylene furanoate) (PEF) by a two-stage melt polymerization procedure. Their catalytic performance was compared to conventional metal catalysts such as Sb_2O_3 Bu_2SnO, and $Ti(OnBu)_4$. Al/Sn/Al-based LDH04, Mg/Al/Ti-based LDH10, and Mg/Al-based commercial hydrotalcite (LDH19) exhibited polymerization rates comparable to those obtained with Sb_2O_3 and Bu_2SnO, as well as the most favourable coloration. Amongst these, commercially available LDH19 achieved the higher molecular weights (Mn and Mw). Additionally, thermal and structural properties, including Tg and TGA results, were evaluated, demonstrating competitive performance. The scalability of LDH-based catalysis was confirmed through a 30-gram scale polymerization. The versatility of LDHs was further validated by synthesising furan-based polyesters with different diol chain lengths, whose structures were confirmed by ^{1}H NMR. These findings highlight the potential of LDHs as sustainable catalysts for the production of biobased furanoate polyesters, advancing the field toward greener polymerization processes.

Acknowledgements

This Special Issue is dedicated to honor the 5th International Symposium on Catalysis for Clean Energy and Sustainable Chemistry (CCESC 2024). The authors thank the Instituto Valenciano de

Competitividad Empresarial (IVACE) in the Comunitat Valenciana for the financial support to the projects CLIMA21 (IMAMCG/2021/1), CLIMA22 (IMAMCA/2022/4) and LÍNEAGVA_QUIMSOST24 (IMAMCA/2024/4). In addition, the authors want to express their gratitude to University of Valencia for the RMN and RX spectra.

Author contributions: CRediT

Daniela Ramírez Espinosa: Investigation, resources, formal analysis, validation, writing-original draft. **Laura Martí Montaner:** Funding acquisition, conceptualization, project administration, supervision, methodology, validation. **Alicia Monleón-Ventura:** Project administration, conceptualization, methodology, investigation, writing-original draft, supervision.

References

[1] V. Siracusa, I. Blanco, Bio-Polyethylene (Bio-PE), Bio-Polypropylene (Bio-PP) and Bio-Poly(ethylene terephthalate) (Bio-PET): Recent Developments in Bio-Based Polymers Analogous to Petroleum-Derived Ones for Packaging and Engineering Applications, Polymers 12 (2020) 1641. https://doi.org/10.3390/polym12081641
[2] E. de Jong, H. (R.) A. Visser, A. Sousa Dias, C. Harvey, G.-J. M. Gruter, The Road to Bring FDCA and PEF to the Market, Polymers 14 (2022) 943. https://doi.org/10.3390/polym14050943
[3] S. K. Burgess, J. E. Leisen, B. E. Kraftschik, C. R. Mubarak, R. M. Kriegel, W. J. Koros, Chain Mobility, Thermal, and Mechanical Properties of Poly(ethylene furanoate) Compared to Poly(ethylene terephthalate), Macromolecules 47 (2014) 1383 – 1391. https://doi.org/10.1021/ma5000199
[4] S. K. Burgess, G. B. Wenz, R. M. Kriegel, W. J. Koros, Penetrant transport in semicrystalline poly(ethylene furanoate), Polymer 98 (2016) 305–310. https://doi.org/10.1016/j.polymer.2016.06.046
[5] M. Zhao, C. Zhang, F. Yang, Y. Weng, Gas barrier properties of furan-based polyester films analyzed experimentally and by molecular simulations, Polymer 233 (2021) 124200 – 9. https://doi.org/10.1016/j.polymer.2021.124200
[6] G. Z. Papageorgiou, D. G. Papageorgiou, Z. Terzopoulou, D. N. Bikiaris, Production of bio-based 2,5-furan dicarboxylate polyesters: Recent progress and critical aspects in their synthesis and thermal properties, Eur. Polym. J. 83 (2016) 202 – 229. https://doi.org/10.1016/j.eurpolymj.2016.08.004
[7] Z. Terzopoulou, L. Papadopoulos, A. Zamboulis, D. G. Papageorgiou, G. Z. Papageorgiou, D. N. Bikiaris, Tuning the Properties of Furandicarboxylic Acid-Based Polyesters with Copolymerization: A Review, Polymers, 12 (2020) 1209. https://doi.org/10.3390/polym12061209
[8] G. Z. Papageorgiou, V. Tsanaktsis, D. N. Bikiaris, Synthesis of poly(ethylene furandicarboxylate) polyester using monomers derived from renewable resources: thermal behavior comparison with PET and PEN, Phys. Chem. Chem. Phys. 16 (2014) 7946 – 7958. https://doi.org/10.1039/C4CP00518J
[9] N. Kasmi, M. Majdoub, G. Z. Papageorgiou, D. S. Achilias, D. N. Bikiaris, Solid-State Polymerization of Poly(ethylene furanoate) Biobased Polyester, I: Effect of Catalyst Type on MolecularWeight Increase, Polymers 9 (2017) 607. https://doi.org/10.3390/polym9110607
[10] EU Directive 2009/425 EC. https://eur-lex.europa.eu/legal-content/EN/TXT/?uri=CELEX%3A32009D0425, 2024 (accessed 9 November 2024).
[11] X.-l. Qu, M. Jiang, B. Wang, J. Deng, R. Wang, Q. Zhang, G.-y. Zhou, J. Tang, A Brønsted Acidic Ionic Liquid as an Efficient and Selective Catalyst System for Bioderived High Molecular Weight Poly(ethylene 2,5-furandicarboxylate), ChemSusChem 12 (2019) 4927 – 4935. https://doi.org/10.1002/cssc.201902020
[12] Q. Zhou, Y. Zhao, Y. Shi, R. Zheng, L. Guo, Acidic Metal-Based Functional Ionic Liquids Catalyze the Synthesis of Bio-Based PEF Polyester, Polymers 16 (2024) 103. https://doi.org/10.3390/polym16010103
[13] K. v. d. Maas, D. H. Weinland, R.-J. v. Putten, B. Wang, G.-J. M. Gruter, Catalyst free PET and PEF polyesters using a new traceless oxalate chain extender, Green Chem. 26 (2024) 11182 – 11195. https://doi.org/10.1039/D4GC02791D
[14] J.-G. Rosenboom, D. K. Hohl, P. Fleckenstein, G. Storti, M. Morbidelli, Bottle-grade polyethylene furanoate from ring-opening polymerisation of cyclic oligomers, Nat. Commun. 9 (2018) 2701. https://doi.org/10.1038/s41467-018-05147-y
[15] M. Hoppe, P. De Voogt, R. Franz, Oligomers in polyethylene furanoate - identification and quantification approach via LC-UV LCMS response ratio, Food Additives & Contaminants: Part A, 35 (2018) 2244 – 2255. https://doi.org/10.1080/19440049.2018.1523576
[16] J.-P. Wiegner, R. Eckert, W. Voerckel, G. Feix, M. Sela, S, Munjal (2004). Catalyst systems for polycondensation reactions (US Patent No. 6,828,272 B2) PCT. https://patents.google.com/patent/US6828272B2/en

[17] M. Kêdzierski, Z. Boñcza-Tomaszewski, G. Jaworska, A. Niska, Layered double hydroxides as transesterification catalysts and nanofillers for polyester resin, Polymery 60 (2015) 160. https://doi.org/10.14314/polimery.2015.160
[18] Z. Feng, Z. Yang, J. Huang, X. Xie, Z. Zhang, Influences of Zn-Sn-Al-hydrotalcite additive on the electrochemical performances of ZnO for zinc-nickel secondary cells. J. Electrochem. Soc. 161 (2014), A1981. https://doi.org/10.1149/2.0191414jes
[19] C. Jiménez-Sanchidrián, J.R. Ruiz, Tin-containing hydrotalcite-like compounds as catalysts for the Meerwein–Ponndorf–Verley reaction. Appl. Catal. A: General 469 (2014) 367 – 372. https://doi.org/10.1016/j.apcata.2013.09.049
[20] U.R. Pillai, E. Sahle-Demessie, Sn-exchanged hydrotalcites as catalysts for clean and selective Baeyer–Villiger oxidation of ketones using hydrogen peroxide, J. Mol. Catal. A: Chemical 191 (2003) 93 – 100. https://doi.org/10.1016/S1381-1169(02)00347-3
[21] S. Velu, K. Suzuki, T. Osaki, F. Ohashi, S. Tomura, Synthesis of new Sn incorporated layered double hydroxides and their evolution to mixed oxides. Mater. Res. Bull. 34 (1999) 1707 – 1717. https://doi.org/10.1016/S0025-5408(99)00168-3
[22] L. Wang, Y. Liu, X. Chen, H. Qin, Z. Yang, Zinc aluminum antimony hydrotalcite as anode materials for Ni-Zn secondary batteries, J. Electrochem. Soc. 164 (2017) A3692 – A3698. https://doi.org/10.1149/2.0831714jes
[23] Y. D. Morcillo-Bolaños, W.J. Malule-Herrera, J.C. Ortiz-Arango, A.L. Villa-Holguín, Polyurethane flexible foam recycling via glycolysis using Zn/Sn/Al hydrotalcites as heterogeneous catalyst, Revista Facultad de Ingeniería Universidad de Antioquia 87 (2018) 77-85. https://doi.org/10.17533/udea.redin.n87a10
[24] T. Wang, Z. Yang, B. Yang, R. Wang, J. Huang, The electrochemical performances of Zn–Sn–Al-hydrotalcites in Zn–Ni secondary cells, J. Power Sources 257 (2014) 174 – 180. https://doi.org/10.1016/j.jpowsour.2014.02.006
[25] O.Saber, H. Tagaya, Preparation and intercalation reactions of nano-structural materials, Zn–Al–Ti LDH. Materials Chemistry and Physics 108.2-3 (2008): 449-455. https://doi.org/10.1016/j.matchemphys.2007.10.024
[26] C. Jiménez-Sanchidrián, J.R. Ruiz, Tin-containing hydrotalcite-like compounds as catalysts for the Meerwein–Ponndorf–Verley reaction. Applied Catalysis A: General 469 (2014): 367 – 372. https://doi.org/10.1016/j.apcata.2013.09.049
[27] O. Saber, H. Tagaya, New layered double hydroxide, Zn–Ti LDH: preparation and intercalation reactions. Journal of inclusion phenomena and macrocyclic chemistry 45 (2003) 107 – 115. https://doi.org/10.1023/A:1023078728942
[28] W.Y. Hernández, F. Aliç, A. Verberckmoes, P. Van Der Voort, Tuning the acidic–basic properties by Zn-substitution in Mg–Al hydrotalcites as optimal catalysts for the aldol condensation reaction, J. of Materials Science 52 (2017) 628 – 642. https://doi.org/10.1007/s10853-016-0360-3
[29] X. Chen, Z. Yang, L.Wang, H. Qin, Synthesis of rose-like ZnAl-LDH and its application in zinc–nickel secondary battery, Nanotechnology 30 (2018) 015602. https://doi.org/10.1088/1361-6528/aae56e
[30] N. Das, N., A. Samal, Synthesis, characterisation and rehydration behaviour of titanium (IV) containing hydrotalcite like compounds. Microporous and mesoporous materials 72.1-3 (2004): 219-225. https://doi.org/10.1016/j.micromeso.2004.04.004
[31] D. Kwon, J. Y. Kang, S. An, I. Yang, J. C. Jung, Tuning the base properties of Mg–Al hydrotalcite catalysts using their memory effect, J. Energy Chem. 46 (2020) 229 – 236. https://doi.org/10.1016/j.jechem.2019.11.013
[32] Shao, M., Han, J., Wei, M., Evans, D. G., & Duan, The synthesis of hierarchical Zn–Ti layered double hydroxide for efficient visible-light photocatalysis. Chemical Engineering Journal 168.2 (2011): 519-524. https://doi.org/10.1016/j.cej.2011.01.016
[33] A. Marshall, B. Jiang, R. M. Gauvin, C. M. Thomas, 2,5-Furandicarboxylic Acid: An Intriguing Precursor for Monomer and Polymer Synthesis, Molecules 27 (2022) 4071. https://doi.org/10.3390/molecules27134071
[34] K. Loos, R. Zhang, I. Pereira, B. Agostinho, H. Hu, D. Maniar, N. Sbirrazzuoli, A. J. D. Silvestre, N. Guigo, A. F. Sousa, A Perspective on PEF Synthesis, Properties, and End-Life, Front. Chem. 8 (2020) a585. https://doi.org/10.3389/fchem.2020.00585
[35] Z. Terzopoulou, E. Karakatsianopoulou, N. Kasmi, V. Tsanaktsis, N. Nikolaidis, M. Kostoglou, G. Z. Papageorgiou, D. A. Lambropouloud, D. N. Bikiaris, Effect of catalyst type on molecular weight increase and coloration of poly(ethylene furanoate) biobased polyester during melt polycondensation, Polym. Chem. 8 (2017) 6895 – 6908. https://doi.org/10.1039/C7PY01171G
[36] M. B. Banella, J. Bonucci, M. Vannini, P. Marchese, C. Lorenzetti, A. Celli, Insights into the Synthesis of Poly(ethylene 2,5-Furandicarboxylate) from 2,5-Furandicarboxylic Acid: Steps toward Environmental and Food Safety Excellence in Packaging Applications, Ind. Eng. Chem. Res. 58 (2019) 8955−8962. https://doi.org/10.1021/acs.iecr.9b00661
[37] Z. Terzopoulou, E. Karakatsianopoulou, N. Kasmi, M. Majdoub, G. Z. Papageorgiou, D. N. Bikiaris, Effect of catalyst type on recyclability and decomposition mechanism of poly(ethylene furanoate) biobased polyester, J. Anal. Appl. Pyrolysis 126 (2017) 357 – 370. https://doi.org/10.1016/j.jaap.2017.05.010
[38] G. G. M. Soccio, M. C. García-Gutiérrez, T. Ezquerra, V. Siracusa, E. Gutiérrez-Fernández, A. Munari, N. Lotti, Fully Biobased Superpolymers of 2,5-Furandicarboxylic Acid with Different Functional Properties: From Rigid to Flexible, High Performant Packaging Materials, ACS Sustainable Chem. Eng. 8 (2020) 9558 – 9568. https://doi.org/10.1021/acssuschemeng.0c02840
[39] V. Tsanaktsis, Z. Terzopoulou, M. Nerantzaki, G. Z. Papageorgiou, D. N. Bikiaris, New poly(pentylene furanoate) and poly(heptylene furanoate) sustainable polyesters from diols with odd methylene groups, Mater. Lett. 178 (2016) 64–67. http://dx.doi.org/10.1016/j.matlet.2016.04.183